

ratio of yields from Pt to Be is 10.8 at 13° , whereas we find a ratio of 25 for Pb to Be at 17° . This difference is larger than the experimental error. On the other hand, their cross section at 32° for Be is 2.3 mb/sr BeV/c, whereas ours is approximately 2.6 mb/sr BeV/c at the peak, which is well within the experimental error.

They agree with us that the production cross section is too large to be explained by a primary process such as $p + p \rightarrow d + \pi^+$, and must, therefore, be nuclear in origin. They also invoke the process suggested by Butler and Pearson.⁶⁻⁸ Their suggestion that the lower part of the momentum spectrum arises from pairing of slower nucleons and nucleons in the tail of the Fermi distribution is similar to the indirect pickup process we suggest is operative. The experiments by Hess¹⁸ indicate this may be large enough to explain the low-energy deuterons.

IV. CONCLUSIONS

Although the exigencies of time and circumstances prevented us from obtaining accurate data, we feel we

can say conclusively that the large deuteron production for protons incident in the region from 1-3 BeV is the result of several processes in which the indirect pickup process plays only a minor part. The deuterons of low momentum probably arise from such a process, but those of high momentum must arise from some other mechanism such as the amalgamation of two nucleons in the cascade. Those of the highest energy come from a quasielastic scattering process with deuterons existing as a result of fluctuations within the nucleus.

ACKNOWLEDGMENTS

The experiments discussed in this paper were performed by F. T. Avignone, R. L. Childers, C. W. Darden, R. D. Edge, and D. W. Tompkins of the University of South Carolina, and J. W. Glenn and several members of the operating staff of the Cosmotron. D. W. Tompkins and J. W. Glenn helped with the analysis of the data. Our thanks are due to members of the Rochester group for assistance and the loan of equipment.

Energy and Angular Dependence of Differential Cross Sections for the $^{16}\text{O}(^{16}\text{O}, \alpha)^{28}\text{Si}$ Reaction*

R. W. SHAW, JR., J. C. NORMAN,† R. VANDENBOSCH, AND C. J. BISHOP
Department of Chemistry, University of Washington, Seattle, Washington 98105
 (Received 6 January 1969)

Excitation functions for elastic scattering and α -particle emission have been measured for 35-39-MeV oxygen projectiles incident on an oxygen target. Differential cross sections for α -particle emission to the ground and first excited states of ^{28}Si are approximately 10-100 $\mu\text{b}/\text{sr}$. The angular distribution at 36-MeV laboratory bombarding energy indicates that $J=12$ angular momentum states of the compound nucleus are the dominant contributors for α decay to the ^{28}Si ground state. The fluctuation width obtained from both the elastic and the α -particle-emission channel is 76 ± 17 keV. Neither the fine nor gross structure in the elastic scattering excitation function is correlated with fluctuations in the cross section for α -particle emission from the compound nucleus. The level density of spin-12 states of the ^{28}S compound nucleus at an excitation energy of 34.2 MeV has been determined to be 2000 levels per MeV. Statistical-model calculations of the level density, average cross sections, and fluctuation widths require a value of the nuclear level-density parameter a between $A/7$ and $A/9$.

I. INTRODUCTION

MEASUREMENTS of the energy and angular dependence of differential cross sections for compound-nuclear reactions enable one to extract useful information about nuclear level densities and nuclear lifetimes.¹⁻⁴ Angular momentum effects associated with

heavy ion reactions⁵⁻⁷ between identical spin-zero particles make it possible to extract more specific information than is usually obtained from cross-section studies. This is because only even-spin even-parity compound nuclei are formed; and it is possible to select exit channels which are fed by only one or, at most, a few spin states of the compound nucleus. The angular momentum of the compound states making the principal contribution to a particular exit channel can be determined from the angular distribution for this exit

* Work supported in part by the U.S. Atomic Energy Commission.

† Present address: Department of Chemistry, University of Wisconsin, Green Bay, Wis.

¹ A. Richter, W. Von Witsch, P. von Brentano, O. Häusser, and T. Mayer-Kuckuk, *Phys. Letters* **14**, 121 (1965).

² J. R. Huizenga, A. A. Katsanos, and H. K. Vonach, *Bull. Am. Phys. Soc.* **11**, 365 (1966).

³ R. Vandenbosch, J. C. Norman, and C. J. Bishop, *Phys. Rev.* **158**, 887 (1967).

⁴ A. A. Katsanos, Argonne National Laboratory Report No. ANL 7289 (unpublished).

⁵ E. Almqvist, J. A. Kuehner, D. McPherson, and E. W. Vogt, *Phys. Rev.* **136**, B84 (1964).

⁶ E. W. Vogt, D. McPherson, J. Kuehner, and E. Almqvist, *Phys. Rev.* **136**, B99 (1964).

⁷ J. P. Bondorf and R. B. Leachman, *Kgl. Danske Videnskab. Selskab, Mat.-Fys. Medd.* **34**, No. 10 (1965).

channel. A fluctuation analysis of a thin-target excitation function then enables one to determine the average compound-nuclear width for a known angular momentum. Comparison of the absolute average cross sections and the widths with statistical-model calculations enables one to extract information about the angular momentum and energy dependence of nuclear level densities.

We have studied the $^{16}\text{O}(^{16}\text{O}, \alpha)^{28}\text{Si}$ reaction for bombarding energies between 35 and 39 MeV. We had hoped to perform fluctuation studies at appreciably higher energies corresponding to the excitation energy in a previous study³ of the inverse reaction $^{28}\text{Si}(\alpha, ^{16}\text{O})^{16}\text{O}$ at an α -particle energy of 42 MeV. The energy region studied is, however, higher than has been investigated previously. The same compound nucleus has been studied at lower excitation energies by the $^{31}\text{P}(p, \alpha)^{28}\text{Si}$ reaction by Katsanos⁴ and by Leachman and Fessenden,⁸ and by the $^{16}\text{O}(^{16}\text{O}, \alpha)^{28}\text{Si}$ reaction.⁸

Recently, Siemssen *et al.*⁹ have reported structure in the excitation function for $^{16}\text{O}+^{16}\text{O}$ elastic scattering. The excitation function exhibits gross structure with a periodicity of approximately 4 MeV in the center-of-mass (c.m.) system. There is some evidence of fine structure in this data. We have repeated the elastic measurements at smaller energy increments to look for possible correlations between the elastic and $^4\text{He}+^{28}\text{Si}$ exit channels in either the fine or gross structure.

II. EXPERIMENTAL ARRANGEMENT AND RESULTS

A beam of singly-charged negative ^{16}O ions was produced in the negative-ion source of the University of Washington tandem Van de Graaff accelerator from a mixture of hydrogen and oxygen gases with a BaO-coated Pt-mesh filament. After the stripping of two or more electrons by oxygen gas at the high-voltage terminal and the final stage of acceleration, the beam was magnetically analyzed to obtain only the desired charge state (+5 or +6, depending on the energy desired). The collimated beam then impinged on either a self-supporting NiO target ($\sim 200 \mu\text{g}/\text{cm}^2$) or a target of WO_3 ($\sim 30 \mu\text{g}/\text{cm}^2$) evaporated onto an Au foil. A target of WO_3 on Au ($\sim 15 \mu\text{g}/\text{cm}^2$) was used in the elastic scattering measurements. Finally, the ^{16}O ion beam was collected in a Faraday cup and the beam current electronically integrated. The average effective charge of the ^{16}O ions after passing through the target was calculated from the empirical relationships of Northcliffe,¹⁰ from the data of Bernard *et al.*,¹¹ and from comparison of the beam current with the target in place

to that observed with no target. The three methods agreed to better than $\pm 5\%$.

Silicon particle detectors of the lithium-drifted and surface-barrier types were used to detect the α particles and the elastically scattered oxygen ions. The α -particle detectors were collimated with circular apertures such that they subtended an angle $\Delta\theta_{\text{lab}} = 3.0^\circ$ in the reaction plane and a solid angle $\Delta\Omega_{\text{lab}} = 2 \times 10^{-3}$ sr. The collimators were covered by $\sim 10 \text{ mg}/\text{cm}^2$ of aluminum foil which served to stop the scattered ^{16}O beam and as a support for a ^{212}Pb - ^{212}Bi - ^{212}Po α source which provided a continuous energy calibration standard. A coincidence technique was employed in the elastic scattering measurements. The angle-defining oxygen detector subtended 4.1° . Another unshielded detector was used to monitor the scattered ^{16}O beam. Comparison of elastic scattering data with that of Bromley *et al.*¹² was used to confirm the estimates of target thickness. The signals from the detectors were, after suitable amplification, either presented to conventional pulse-height analyzers or to an SDS 930 computer operated in a real-time mode as four 256-channel pulse-height analyzers. Only α -particle groups corresponding to formation of the residual ^{28}Si nucleus in the 0^+ ground state and the 1.78-MeV 2^+ first excited state were completely resolved.

The measurements were of three types: (a) The excitation functions for the reactions $^{16}\text{O}(^{16}\text{O}, ^4\text{He})^{28}\text{Si}$ (g.s., 0^+) and $^{16}\text{O}(^{16}\text{O}, ^4\text{He})^{28}\text{Si}$ (1.78 MeV, 2^+) were determined in 100-keV increments of the laboratory energy of the oxygen projectiles, corresponding to 50-keV increments in the c.m. system. Detectors were placed at $+13^\circ$ c.m., -13° c.m., $+26^\circ$ c.m., and -26° c.m. with the WO_3 target perpendicular to the beam. The energy resolution was approximately 60 keV in the c.m. system, due mainly to energy loss in the target. The results given in Fig. 1 include the sums of the counts from both detectors at equal angles with respect to the beam. (b) Angular distributions of the emitted α particles were taken at 36.0-MeV incident ^{16}O ion energy (in the laboratory system). The angular distribution was determined with the NiO target at 45° in the laboratory system with respect to the beam (giving an effective target thickness of 1.3 MeV) and four independent detectors. The results are shown in Fig. 2. (c) The excitation function for ^{16}O - ^{16}O elastic scattering was determined in 100-keV increments of the laboratory energy of the oxygen projectiles. Detectors were placed at 90° c.m. with the WO_3 target perpendicular to the beam. The energy resolution was approximately 35 keV in the c.m. system. The results are given in Fig. 1.

The errors indicated in Figs. 1 and 2 are those due only to the statistical uncertainty in the number of counts recorded. The systematic error, due mainly to uncertainties in the target thickness and average charge of the ^{16}O ion beam, is believed to be less than 20%.

¹² D. A. Bromley, J. A. Kuehner, and E. Almqvist, *Phys. Rev.* **123**, 878 (1961).

⁸ R. B. Leachman and P. Fessenden, *Bull. Am. Phys. Soc.* **12**, 206 (1967).

⁹ R. H. Siemssen, J. V. Maher, A. Weidinger, and D. A. Bromley, *Phys. Rev. Letters* **19**, 369 (1967).

¹⁰ L. C. Northcliffe, *Ann. Rev. Nucl. Sci.* **13**, 69 (1963).

¹¹ D. L. Bernard, B. E. Bonner, G. C. Phillips, and P. H. Stelson, *Nucl. Phys.* **73**, 513 (1955).

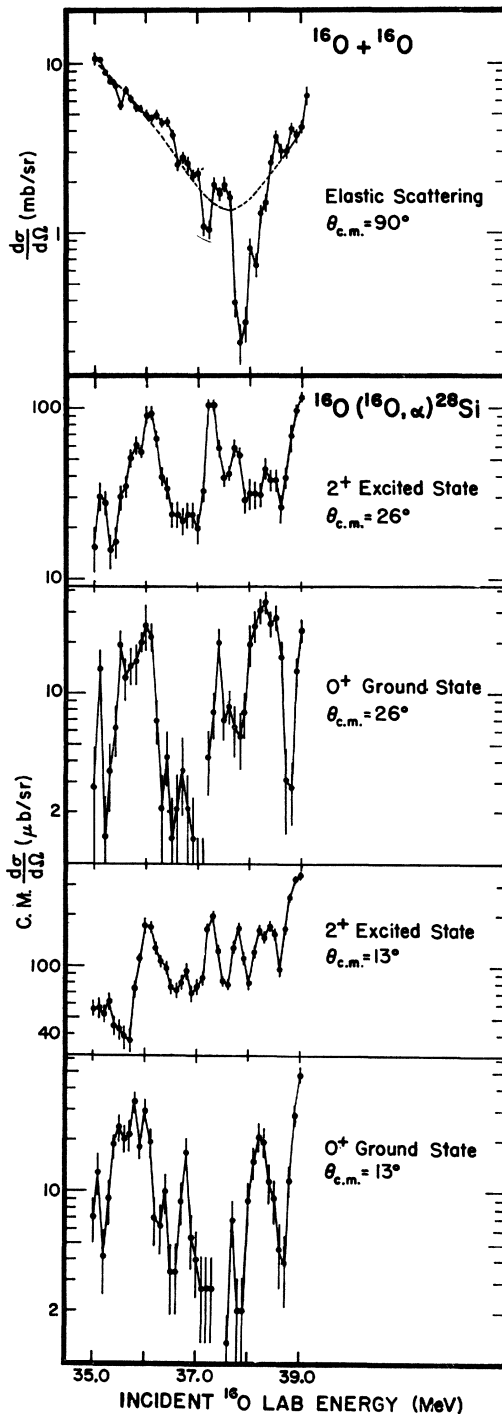


FIG. 1. The excitation functions for the reaction $^{16}\text{O}(^{16}\text{O}, \alpha)^{28}\text{Si}$ leading to the ground state and first excited state of ^{28}Si at 13° c.m. and 26° c.m. and for $^{16}\text{O}+^{16}\text{O}$ elastic scattering at 90° c.m. The solid curves are drawn solely to guide the eye. The dashed line superimposed on the elastic scattering data is a fit with a function quadratic in energy (see Sec. IV).

III. FLUCTUATION ANALYSIS OF $^{16}\text{O}(^{16}\text{O}, \alpha)^{28}\text{Si}$ REACTION

A. Autocorrelations

There are several inconsistencies in the literature concerning the procedure for extracting compound-nucleus widths from excitation-function data which exhibit Ericson fluctuations. The following method is based largely on the theoretical development of Gibbs¹³:

The autocorrelation function may be defined as

$$R'(\epsilon) = \frac{\langle \sigma(E)\sigma(E+\epsilon) \rangle}{\langle \sigma(E) \rangle^2} - 1 = \frac{(1 - Y_D^2)\Gamma^2}{N(\Gamma^2 + \epsilon^2)}, \quad (1)$$

where $\sigma(E)$ is the cross section for a given exit channel at excitation energy E , ϵ is a variable energy increment, N is the number of independent substates for the channel of interest, Y_D is the ratio of direct to total reaction cross section, and Γ is the coherence width. One may determine Γ in two ways from the autocorrelation functions: (a) from the shape of $R(\epsilon)$, and (b) from the absolute value of $R(\epsilon)$. In this experiment, a shape analysis was carried out to determine Γ . This Γ and the

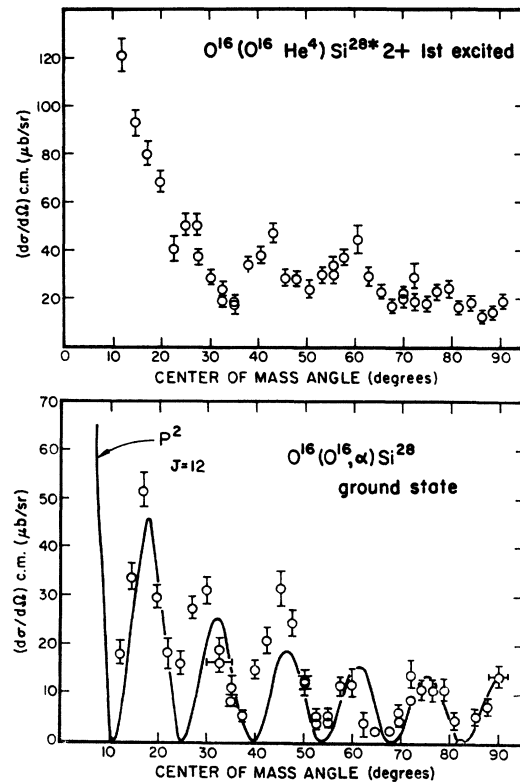


FIG. 2. The experimental angular distributions at 36.0 MeV ^{16}O projectile laboratory energy. The solid line is the square of the Legendre polynomial of order 12.

¹³ W. R. Gibbs, Los Alamos Scientific Laboratory Report No. LA-3266 (unpublished).

TABLE I. Summary of autocorrelation analysis. The third column gives the widths determined from the shape of the autocorrelation function corrected for counting statistics and resolution. The fourth column gives the width after correction for FRD. The fifth and seventh columns give the autocorrelation coefficients before and after FRD correction. The sixth column gives the number N of independent substates. The final column gives the percent of direct reaction implied by combining Γ_0 and $R(0)$, together with the standard deviation associated with the FRD uncertainty. The average excitation energy of the ^{28}S compound nucleus is 35.0 MeV.

$\theta_{\text{c.m.}}$	Level	Γ_{exp}	Γ_0	$R(0)_{\text{exp}}$	N	$R(0)_{\text{corr}}$	Y_D
13°	0 ⁺ g.s.	55	54±11	0.768	1	0.863±0.330	0.37 _{-0.37} ^{+0.31}
26°	0 ⁺ g.s.	95	113±30	0.690	1	0.848±0.423	0.39 _{-0.38} ^{+0.37}
13°	2 ⁺	60	69±14	0.337	1.45	0.633±0.239	0.61 _{-0.28} ^{+0.17}
26°	2 ⁺	55	67±12	0.338	2.22	0.902±0.319	0.32 _{-0.32} ^{+0.33}
av			76±17				
90°	elastic ^a	65	77±17	0.104	1	0.125±0.054	0.936 _{-0.028} ^{+0.028}

^a Modulation corrected, see text.

absolute magnitude of $R(\epsilon)$ were then used to determine Y_D .

To determine the true coherence width Γ^0 from the observed width Γ , three corrections have been made in the course of this analysis: (a) counting statistics, (b) resolution, (c) finite range of data (FRD). $R'(0)$ must be corrected for the effect of counting statistics according to

$$R(0) = R'(0) - \bar{n}^{-1}, \quad (2)$$

where \bar{n} is the average number of counts recorded at each energy. This correction was 6% or less.

The expression given by Dearnaley *et al.*¹⁴ for correction of experimentally determined cross sections for finite energy resolution was adopted because of the convenience of the resolution-corrected cross sections in making cross-correlation calculations described below. In general, this correction changed the cross section by less than 10%.

FRD corrections were calculated using two expressions by Gibbs.^{15,16} These agreed to well within their uncertainties and the simpler one¹⁶ was adopted for convenience:

$$\Gamma^0/\Gamma = \left(\frac{N(n-1)}{N(n+1)+2} \right)^{1/2}, \quad (3)$$

where n is the independent sample size¹³ and is given by

$$n = (I/\pi\Gamma) + 1. \quad (4)$$

Here, I is the excitation energy interval over which the cross section is averaged. The dependence of $R(0)$ on the sample size and the number of independent substates is given by¹⁷

$$R(0) = (n-1)/(1+nN). \quad (5)$$

The relative standard deviation (RSD) of $R(0)$ and Γ due to FRD are given by¹⁸

$$\text{RSD}[R(0)] = [(1+1/N)/n]^{1/2}, \quad (6)$$

$$\text{RSD}[\Gamma] = [(1+1/N)/4I/\pi\Gamma]^{1/2}. \quad (7)$$

The sample size n in these measurements ranges from 8 to 14, and the FRD correction from 10 to 20%. The coherence widths Γ^0 deduced from the shape of the autocorrelation function after correction for counting statistics, resolution, and FRD are given in Table I. The uncertainties are the predicted standard deviations expected from the small sample size and do not include statistical uncertainties, resolution uncertainties, or the uncertainty in defining the width from the shape of the autocorrelation function. An expression by Bohning¹⁹ for this last uncertainty gives an error ranging from ±26 to ±37% using the sample sizes in this experiment. An analysis of synthetic excitation functions by VanderWoude²⁰ gives ±15–±22%.

The shape analysis of $R(\epsilon)$ does not depend on Y_D or N . One may, therefore, determine FRD and resolution corrections from the shape-analysis value of Γ^0 , apply these corrections to $R(0)$ and, knowing N , calculate Y_D from the absolute magnitude of $R(0)$. For the reaction to the zero-spin ground state, $N=1$. The effective value of N for the 2⁺ excited state is a complicated function of angle and can have a maximum value of 3. Richter has performed calculations to determine the effective number of contributing substates N_{eff} for the 2⁺ excited state. At 13° c.m. and 26° c.m., N_{eff} is 1.54 and 2.22, respectively.²¹ The experimental values of $R(0)$ corrected for resolution, counting statistics, and

¹⁴ G. Dearnaley, W. R. Gibbs, R. B. Leachman, and P. C. Rogers, *Phys. Rev.* **139**, B1176 (1965).

¹⁵ See Eq. (30) of Ref. 13.

¹⁶ M. L. Halbert, F. E. Durham, and A. VanderWoude, *Phys. Rev.* **162**, 899 (1967); see Eq. (B13).

¹⁷ See Eq. (B7) of Ref. 16.

¹⁸ See Eqs. (B10) and (B19) of Ref. 16.

¹⁹ B. W. Allardyce, P. J. Dallimore, I. Hall, N. W. Tanner, A. Richter, P. von Brentano, and T. Mayer-Kuckuk, *Nucl. Phys.* **85**, 193 (1966); See Eq. (12).

²⁰ A. VanderWoude, *Nucl. Phys.* **80**, 14 (1966); see Fig. 15.

²¹ We are indebted to Dr. Achim Richter for performing these calculations.

normalized to $N=1$, are given in Table I with their FRD uncertainties. The values of Y_D corresponding to the corrected values of $R(0)$ are also given in Table I.

Closed expressions for the FRD corrections have been derived only for the special case $Y_D=0$. We have used these expressions for an initial FRD correction of $R(0)$ and then extracted Y_D from the corrected $R(0)$. Determinations of Y_D were also made using the results of Monte Carlo calculations for $R(0)$ with $Y_D \neq 0$ by Gibbs.¹³ The values of Y_D derived from these calculations agreed to within 6% to 15% of those determined using the closed expressions for FRD corrections. We have, therefore, used the closed expressions [Eqs. (3), (5)–(7)] for simplicity.

Cross-section distributions are shown in Fig. 3 along with the χ^2 distributions of $2N$ degrees of freedom and $Y_D=0$. The distribution corrected for FRD¹³ is only slightly different. The 0^+ ground-state experimental distribution is consistent with the $Y_D=0$ theoretical distribution. The 2^+ excited state distribution shows a peaking about $\sigma/\bar{\sigma}=1$ which indicates that the assumed N values in the theoretical distribution are too small, or that $Y_D > 0$, or both.

B. Cross Correlations between Final States

Statistical theory predicts that transitions to different final states are uncorrelated. The symmetrized cross correlation

$$R^{ij}(\epsilon) = \frac{1}{2} \frac{[\langle \sigma_i(E+\epsilon) - \langle \sigma_i \rangle][\langle \sigma_j(E) - \langle \sigma_j \rangle]}{\langle \sigma_i \rangle \langle \sigma_j \rangle} + \frac{1}{2} \frac{[\langle \sigma_i(E) - \langle \sigma_i \rangle][\langle \sigma_j(E+\epsilon) - \langle \sigma_j \rangle]}{\langle \sigma_i \rangle \langle \sigma_j \rangle}, \quad (8)$$

between two final states i and j , has been evaluated for the ground-state-excited-state pair at the two angles. The observed values for $R^{ij}(0)$ are $+0.20 \pm 0.12$ at 13° c.m. and 0.13 ± 0.13 at 26° c.m. Uncertainties due to the small sample size have been estimated according to relations given by Allardyce *et al.*²² The cross-correlation functions at 13° and at 26° have Gaussian shapes and full width at half-maximum (FWHM) of 45 and 50 keV, respectively, and are large enough to be apparent in the excitation functions (Fig. 1). To exhibit the correlation effects it is convenient to remove the finite sample and independent substate effects by defining a normalized cross-correlation function

$$R_{ij}^N(\epsilon) = R_{ij}(\epsilon) / (R_i(\epsilon) R_j(\epsilon))^{1/2}, \quad (9)$$

which will be equal to unity if transitions to the two states are completely correlated, will be equal to zero if no correlation exists and will be less than zero if anticorrelated. The observed values for $R^N(0)$ are 0.39 ± 0.24 at 13° and 0.27 ± 0.27 at 26° . Although the sample-

size uncertainties are too large to permit any definite conclusions to be drawn from these results, there appears to be some evidence of a positive correlation between the yields of the ground and excited states.

C. Angular Cross Correlations

The angular cross-correlation function is given by

$$R(\theta, \theta') = \frac{\langle \sigma(E, \theta) \sigma(E, \theta') \rangle}{\langle \sigma(E, \theta) \rangle \langle \sigma(E, \theta') \rangle} - 1. \quad (10)$$

As in Sec. III B, it is convenient to use a normalized cross-correlation function

$$R^N(\theta, \theta') = \frac{R(\theta, \theta')}{[R(\theta, \theta) R(\theta', \theta')]^{1/2}}. \quad (11)$$

The normalized angular cross-correlation function $R^N(13^\circ, 26^\circ)$ has a value of 0.58 for the ground state and a value of 0.78 for the first excited state. Brink *et al.*²³ have shown that the differential cross sections should in general be strongly correlated only if $(\theta - \theta')$ is less (in radians) than $(kR)^{-1}$, where k is the wave number of the incident projectile, and R is the nuclear radius. For the system of interest, $(kR)^{-1}$ is equivalent to 11° which, if taken as the half-width at half-maximum, would predict a value of less than 0.5 for $R^N(13^\circ, 26^\circ)$. If, however, compound states with a single J value contribute, the expected value of $R^N(13^\circ, 26^\circ)$ is unity for any pair of angles. The large experimental values of $R^N(13^\circ, 26^\circ)$ indicate that only high-spin compound states with one or two J values are con-

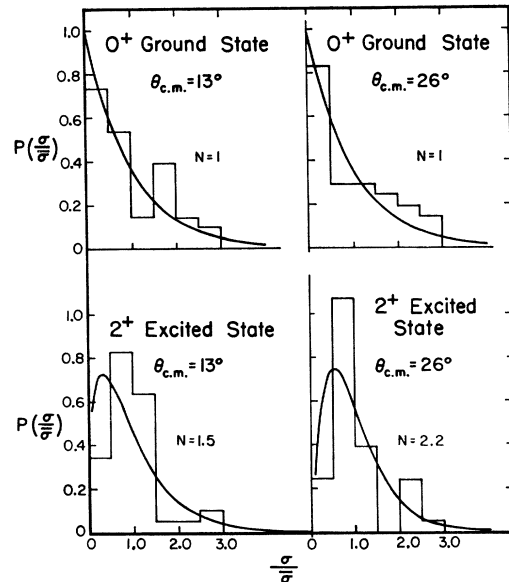


FIG. 3. The probability distribution for the ratio of cross section to average cross section for the reaction leading to the ground state and first excited states of ^{28}Si at 13° c.m. and 26° c.m. The curves are χ^2 distribution of $2N$ degrees of freedom.

²³ D. M. Brink, R. O. Stephen, and N. W. Tanner, Nucl. Phys. **54**, 577 (1964).

²² See Eq. (15) of Ref. 19.

tributing. The angular distribution for producing ^{28}Si in its ground state (Fig. 2) also is indicative of the predominance of a single compound spin state. These indications are further supported by statistical-model calculations described in Sec. VI E.

IV. FLUCTUATION ANALYSIS OF ELASTIC SCATTERING CROSS SECTIONS

Visual inspection of the excitation functions for the $^{28}\text{Si}+^4\text{He}$ and elastic exit channels does not reveal any obvious correlations between elastic and α -particle channels. A more quantitative test was obtained by computing cross-correlation coefficients between the elastic and each of the four α -particle exit-channel excitation functions. The cross-correlation coefficients given in Table II are generally smaller than for the ground-state-first-excited-state cross correlations (see Sec. III) and are more often negative than positive. Because the elastic cross-section excitation function exhibits a periodic gross structure, an attempt was made to remove this modulation by fitting the excitation function with a function quadratic in energy ($a+bE+cE^2$) and recalculating the cross-correlation coefficients with the modulation-corrected elastic excitation function. This quadratic modulation is shown by the dashed line in Fig. 1. The resulting cross-correlation coefficients given in Table II are between -0.02 and $+0.01$, indicating no significant cross correlations for widths small compared to the gross modulation widths of several MeV.

To look more quantitatively for cross correlations in the gross structure, the experimental cross sections at

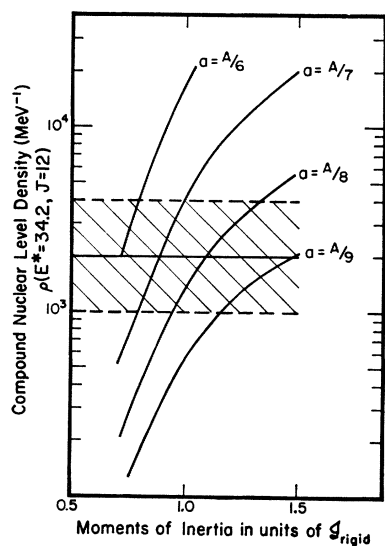


FIG. 4. The horizontal line is the experimentally determined level density and the cross-hatched region corresponds to an estimate of the uncertainty in this determination. The full curves are Fermi gas level densities plotted as a function of I/I_{rigid} for particular values of the level-density parameter a .

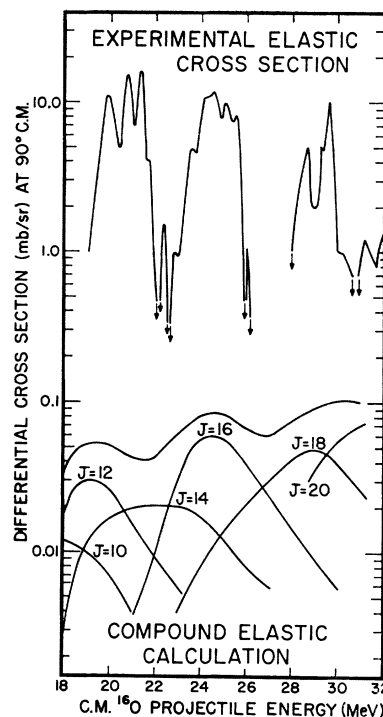


FIG. 5. The lower curves give the calculated partial differential cross sections at 90° c.m. arising from different values of the compound-nucleus angular momentum and the total differential compound elastic cross section. In the upper part of the figure, the experimental results of Siemssen *et al.* (See Ref. 9) are shown. In some energy regions, it was not possible to deduce the cross sections due to the linear presentation of the data published by Siemssen *et al.*

50-keV intervals were averaged over 200-keV intervals and the cross correlation coefficients for all cases were recalculated. The results are given in Table II. The gross structure correlations are roughly equivalent to those calculated with the experimental elastic cross sections as is expected since the large modulations tend to overwhelm the fine structure in the cross-correlation expression. Again no evidence for a positive cross correlation was obtained. We have, therefore, failed to obtain any evidence for cross correlations between the α particle and elastically scattered oxygen channels in either the fine or gross structure which might be indicative of an entrance channel effect.

The autocorrelation function for modulation-corrected elastic scattering excitation function yields a fluctuation width of 77 keV (see Table I) in good agreement with the values obtained from the α exit-channel cross-section fluctuations. The damping of the fluctuations indicates that less than 10% of the elastic cross section at 90° c.m. is compound nuclear. This is consistent with a statistical-model calculation, described below in Sec. VI C, which indicates that less than 10% of the observed cross section at 90° c.m. can be attributed to compound elastic.

TABLE II. Summary of cross-correlation analysis. $\Delta\epsilon$ is the step size in the excitation function. For $\Delta\epsilon=200$ the raw data with $\Delta\epsilon=50$ have been averaged over 200-keV bins. R_{jj}^N is the normalized value.

	R_{jj}	R_{jj}^N
$\alpha_0^+-\alpha_2^+$		
13°, $\Delta\epsilon=50$ keV	0.20±0.12	0.39±0.24
26°, $\Delta\epsilon=50$ keV	0.13±0.13	0.27±0.27
13°, $\Delta\epsilon=200$ keV	0.072	
26°, $\Delta\epsilon=200$ keV	0.052	
α_0^+ -elastic		
13° α_0^+ 90° elas, $\Delta\epsilon=50$	0.183	0.301
26° α_0^+ 90° elas, $\Delta\epsilon=50$	-0.048	-0.084
13° α_0^+ 90° elas, $\Delta\epsilon=50^a$	0.002	0.007
26° α_0^+ 90° elas, $\Delta\epsilon=50^a$	-0.019	-0.072
13° α_0^+ 90° elas, $\Delta\epsilon=200$ keV	0.208	
26° α_0^+ 90° elas, $\Delta\epsilon=200$ keV	-0.040	
α_2^+ -elastic		
13° α_2^+ 90° elas, $\Delta\epsilon=50$ keV	-0.091	-0.220
26° α_2^+ 90° elas, $\Delta\epsilon=50$ keV	-0.058	-0.140
13° α_2^+ 90° elas, $\Delta\epsilon=50^a$	0.008	0.042
26° α_2^+ 90° elas, $\Delta\epsilon=50^a$	0.011	0.058
13° α_2^+ 90° elas, $\Delta\epsilon=200$ keV	-0.107	
26° α_2^+ 90° elas, $\Delta\epsilon=200$ keV	-0.037	

^a Modulation-corrected: gross structure (of order of 1 MeV) removed.

V. DETERMINATION OF LEVEL DENSITY BY COMBINING FLUCTUATION WIDTH WITH AVERAGE CROSS SECTION

Richter *et al.*¹ and Huizenga *et al.*² have shown how it is possible to obtain absolute nuclear level densities by combining fluctuation widths and average cross sections. In the general case, a model for the angular momentum dependence of the level density and the width Γ must be introduced. If, as may be the case in certain heavy ion reactions, only compound states of a single angular momentum value contribute to a particular exit channel, it is possible to deduce the level density for that particular angular momentum and the excitation energy of the compound nucleus. The only other input data required are the transmission coefficients for the incoming and outgoing particles. For identical particles in the entrance channel and spinless particles in all channels, the following relationship can be obtained for the differential cross section from a particular compound angular momentum state J :

$$\frac{d\sigma}{d\Omega}(\theta) = \frac{\lambda^2 T_0^J T_s^J (2J+1)^2 P_J^2(\cos\theta)}{4\pi\Gamma(\frac{1}{2}\rho(E^*, J))}, \quad (11)$$

where T_0^J and T_s^J are the entrance- and exit-channel transmission coefficients, Γ is the fluctuation width,

and $\frac{1}{2}\rho(E^*, J)$ is the compound-nuclear level density for a particular parity. The angular distribution and its statistical-model fit (see Sec. VI E) at $E_{lab}=36$ MeV indicates that the ground state of ^{28}Si is formed primarily from $J=12$ compound-nuclear states. Using the experimental cross section at 90° c.m. and the experimental width Γ of 76 keV, one obtains a level density $\rho(E^*=34.2, J=12)=2.0\times 10^8$ for the compound nucleus ^{32}S . We estimate a standard deviation corresponding to an uncertainty of approximately a factor of 2 in this number, including uncertainties in the transmission coefficients, cross section, coherence width, and fraction of cross section originating from $J=12$ levels.

VI. STATISTICAL-MODEL CALCULATIONS

A. Introduction

Calculations of the compound-nuclear level density, average width of the compound-nuclear states, and average cross sections to given final states were carried out within the framework of the Wolfenstein-Hauser-Feshbach model.²⁴ Transmission coefficients were obtained from optical potentials discussed in Ref. 3. At the high excitation energies under consideration the large number of compound states and available final states, corresponding to the competing exit channels, are most conveniently described by level-density expressions. We have chosen a simple Fermi gas model for the level density. Calculations have been carried out using the same parameterization for residual and compound nuclear level densities except for the moment of inertia \mathcal{I} as described below.

B. Level Density of ^{32}S Compound Nucleus

The nuclear level density has been predicted theoretically to be of the form²⁵

$$\rho(U, J) = \frac{(2J+1)}{12a^{1/4}(U+t)^{5/4}(2\sigma^2)^{3/2}} \exp 2(aU)^{1/2} \times \exp \frac{-(J+\frac{1}{2})^2}{2\sigma^2}, \quad (12)$$

where t is obtained from $U=at^2-t$ and $\sigma^2=gt/h$. We follow the conventional practice of defining the excitation energy $U=E^*-b\delta$, where $b=2$ for $e-e$, 1 for $o-e$, and zero for $o-o$ nuclei. The pairing energy parameter δ was taken as 1.8 MeV, which is the average of the neutron and proton pairing parameters of Nemirovsky and Adamchuk.²⁶ There is recent evidence²⁷ that this is not a satisfactory procedure for treating the odd-even

²⁴ L. Wolfenstein, Phys. Rev. **82**, 690 (1951); W. Hauser and H. Feshbach, *ibid.* **87**, 366 (1952).

²⁵ D. W. Lang, Nucl. Phys. **42**, 353 (1963).

²⁶ P. E. Nemirovsky and Y. V. Adamchuk, Nucl. Phys. **39**, 551 (1962).

²⁷ A. A. Katsanos, R. W. Shaw, R. Vandenbosch, D. Chamberlin (to be published).

effect, but for the high excitation energies under consideration is probably not seriously in error. The above equation has two unspecified parameters: the level-density parameter a and the moment of inertia \mathcal{I} . In Fig. 4, we exhibit the a and \mathcal{I} combinations consistent with the experimentally determined level density of the compound nucleus ^{32}S for $E^*=34.2$ and $J=12$. The moment of inertia is expressed in units of the rigid-body moment ($\mathcal{I}_r=0.4 mA^2R^2$) for $R=1.2A^{1/3}$ (Fermi), where m is the mass of a nucleon and A is the nuclear mass. For $\mathcal{I}=\mathcal{I}_r$, a values between $A/7$ and $A/8$ are consistent with the experimental value.

C. Compound Elastic Cross Section

A calculation of the compound elastic cross section has been performed for comparison with the estimate of the compound elastic cross section from the fluctuation analysis, and also to explore a suggestion²⁸ that the gross structure in the elastic cross section observed by Siemssen *et al.*⁹ may arise from angular momentum effects in the compound elastic channel. It has been noted²⁸ that the peaks at 21, 25, and 29 MeV c.m. energy occur at the energies where $l=14, 16,$ and 18 partial waves are expected to start contributing to compound-nucleus formation. The angular distributions⁹ show diffraction structure at intermediate angles which are not inconsistent with these angular momenta values.

The compound elastic cross section has been computed using Eq. (11) with an enhancement of a factor of 2 due to the fact that the particles in the exit channel are identical bosons, and an enhancement of another factor of 2 rising from the "width fluctuation correction"²⁹ associated with the identical entrance and exit channels. The level-density parameter used was $a=A/8$ and $\mathcal{I}=\mathcal{I}_r$. The results are shown in Fig. 5. The lower curves give the contribution from each angular momentum value of the compound nucleus as a function of energy and the total compound elastic cross section. It can be seen that there is some modulation associated with the opening of new angular momentum channels. This modulation, however, is somewhat broader than the gross structure observed by Siemssen *et al.*

The absolute magnitude of the calculated compound elastic cross section is too low by at least an order of magnitude. This is qualitatively consistent with the results of our fluctuation analysis (Sec. IV) which indicated that less than 10% of the elastic cross section was due to compound elastic in the energy range 17.5–19.5 MeV c.m. There is some evidence, however, that the compound elastic cross section is larger than predicted. This can be seen more clearly by comparing the experimental ratio of the compound elastic cross section to the ground-state α cross section with the calculated ratio of these cross sections. This calculation

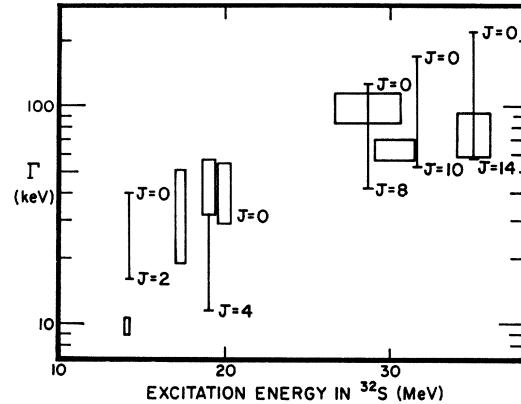


FIG. 6. Calculated and experimental compound-nuclear level widths. The widths measured over the ranges 13.9–14.2 MeV (Ref. 8), 17.0–20.3 MeV (Ref. 4), and 26.7–30.6 MeV (Ref. 8) are from $^{31}\text{P}(p, \alpha)^{28}\text{Si}$ reactions. Those over 29.0–31.4 MeV (Ref. 8) and 34.0–36.0 MeV (this work) from $^{16}\text{O}(^{16}\text{O}, \alpha)^{28}\text{Si}$ reactions. The input parameters were set at $a=A/8$; and $\mathcal{I}=\mathcal{I}_r$ for the compound states and $\mathcal{I}=0.75\mathcal{I}_r$ for the residual states.

is independent of the number of competing channels and hence of the level-density expression. The experimental ratio is 4 ± 2 times larger than the calculated ratio, when only the fluctuation analysis FRD error is included. Additional uncertainties are associated with the removal of the modulation in the fluctuation analysis, and errors in the transmission coefficients used in the calculation. There is, therefore, some indication of enhancement of the compound elastic cross section; but this effect is not certain. It is interesting to note that enhancement of the compound elastic cross section has also been reported in the $^{12}\text{C}+^{12}\text{C}$ system.³⁰

D. Average Compound-Nuclear Level Width

One may write the level width of a compound nucleus at excitation energy E and spin J as

$$\Gamma(E, J) = [2\pi\rho_e(E, J)]^{-1} \sum_{\alpha'} \sum_{I, i, E'} \times \sum_{S=|I-i|}^{I+1} \sum_{l=|J-S|}^{J+S} T_l(\alpha', E'), \quad (13)$$

where $\rho_e(E, J)$ is the compound-nuclear level density, α' labels the kind of particle emitted; and $I, i,$ and S are the residual nuclear spin, the emitted particle spin, and the channel spin, respectively. J is the spin of the compound nucleus, and l is the relative orbital angular momentum of the reaction products. $T_l(\alpha', E')$ is the transmission coefficient for the particle α' in a partial wave of angular momentum l and energy E' .

Using the residual nuclear level density $\rho_R(\alpha', E', I)$

²⁸ J. P. Bondorf and P. von Brenan (private communication).
²⁹ P. A. Moldauer, Phys. Rev. **123**, 968 (1961).

³⁰ E. Almqvist, D. A. Bromley, J. A. Kuehner, and B. Whalen, Phys. Rev. **130**, 1140 (1963).

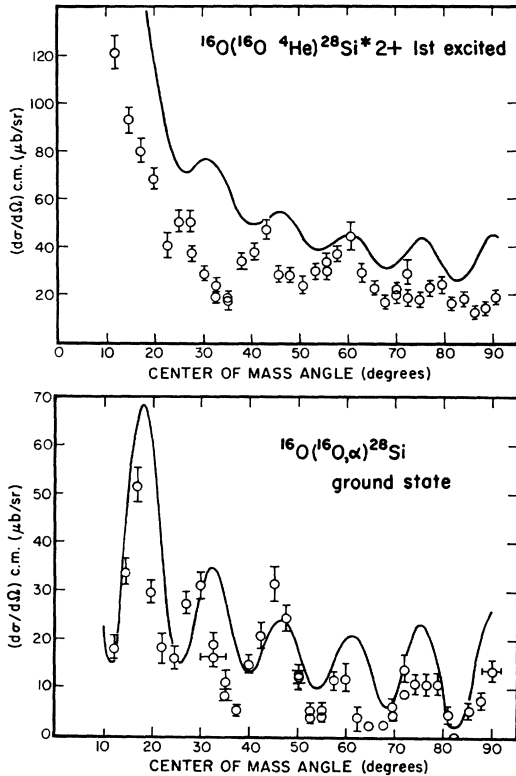


FIG. 7. Experimental angular distributions compared with the statistical-model calculation (solid curve), with $a = A/8$ and $g = g_r$.

to help perform the sums over the T_i 's, we have

$$\Gamma(E, J) = [2\pi\rho_c(E, J)]^{-1} \sum_{\alpha'} \sum_{I, i} \sum_S \sum_l \times \int_E^0 T_l(\alpha', E') \rho_R(\alpha', E'', I) dE'', \quad (14)$$

where $E' + E'' + B_\alpha = E$ and B_α is the separation energy of particle α' . The input parameters are a and g which determine the level densities, and the T_i 's. Equation (14) illustrates the dependence of Γ on both the compound and residual level densities.

Calculations were performed for the α -particle and proton-emission widths Γ_α and Γ_p as a function of E and J of the compound nucleus. The neutron binding energy is nearly twice that for protons or α 's, and Γ_n is negligible. γ emission is also expected to be negligible for the relatively high excitation energy of this experiment.

Two modifications were included in these calculations: (a) States of spin J in the compound or residual nucleus for which an amount of energy corresponding to the rotational energy E_J was greater than the available excitation energy were excluded from the level density. This is equivalent to a recognition of the yrast³¹ levels and prevents a catastrophic increase in

³¹ J. R. Grover, Phys. Rev. **157**, 832 (1967).

the total width at a given J , Γ_J , for high J . E_J was taken to be

$$E_J = J(J+1)\hbar^2/2g. \quad (15)$$

(b) The residual nuclear states known to be within the pairing gap were included in the level density. This increases Γ , but is significant only at low compound-nuclear excitation energies.

Figure 6 shows calculated values of Γ_J and experimental values of Γ^0 from this and other work. The size of the rectangles indicates the experimental range of excitation energy in the compound nucleus and the reported uncertainty in Γ^0 . The extremes of the vertical lines give the calculated Γ^0 for the compound-nuclear angular momenta indicated. The angular momentum range indicated is chosen so as to include all angular momentum states of the compound nucleus involved in the reactions studied.

E. Differential Cross Sections

Minimum χ^2 fits of a function of the form

$$W(\theta) = \sum_{i=0}^{l_{\max}} |A_i P_l(\cos\theta)|^2 \quad (16)$$

have been made to the angular distribution for an incident energy of 36 MeV. The A_i are complex coefficients to be determined by the fitting process; the $P_l(\cos\theta)$ are Legendre polynomials of order l and the sum is over only even values of l since odd angular momentum values are forbidden for a reaction between identical spin-zero nuclei. A value of $l_{\max} = 14$ was found to give a satisfactory fit to the data in each case. However $l_{\max} = 14$ gave only a slightly better fit than $l_{\max} = 12$. These results indicate that the highest spin state of

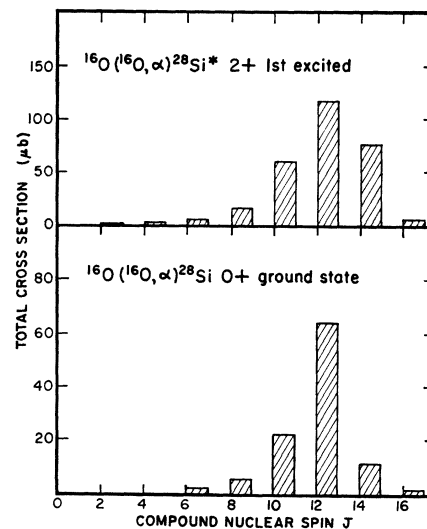


FIG. 8. Calculated contributions of the different compound nuclear spin states to the total cross section as a function of compound-nuclear spin J for the reaction to the 0^+ ground and 2^+ excited states of ^{28}Si .

the compound nucleus making a large contribution to these reaction channels has $J = 12$ with probably a small contribution from $J = 14$ states.

The average differential cross section as a function of c.m. angle (θ) for a reaction in which the target, projectile, and one outgoing particle spin is zero is given by

$$\frac{d\sigma(\alpha, \alpha')}{d\Omega} = \frac{W\lambda^2}{4} \sum_L \sum_{J\pi} T_J(\alpha) \sum_{I'} \frac{T_I(\alpha')}{\sum_{c''} T_{I'}(\alpha'')} \times Z(JJJJ; 0L)Z(WJ; IL) (-1)^I P_L(\cos\theta). \quad (17)$$

This is the general form of Eq. (11). J and π are the total angular momentum and parity, $T_I(\alpha)$ is the transmission coefficient for a pair of particles with orbital angular momentum l , I is the spin of the remaining outgoing particle, the Z 's are the usual Z coefficients, the P_L 's are the Legendre polynomials, W is 2 for even L (or J) and 0 for odd L (or J). The sum over c'' includes all exit channels and is performed, as in Sec. V D, using energy integrals of level-density expressions for the residual states. The yrast modification, described in Sec. VI D, was included in the level-density expressions, but has a negligible effect.

It is possible to extract information about nuclear level densities from the absolute magnitude of the average cross sections, since the cross section for any particular channel depends on the number of competing exit channels. The detailed shape of the calculated angular distribution is sensitive to the optical-model parameters (through the transmission coefficients), whereas the magnitude is largely determined by the statistical-model parameters (through the level densities

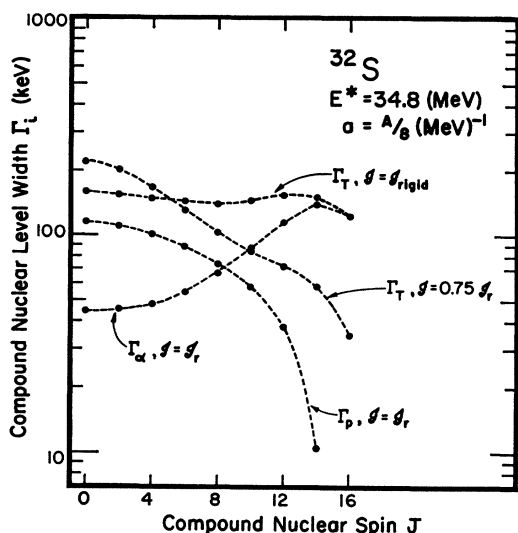


FIG. 9. Calculated dependence of the level width of ^{32}S on the compound-nuclear spin. Γ_α , Γ_p , Γ_T are the total widths for α emission, neutron emission, and their sum, respectively. The compound-nuclear excitation energy is 34.8 MeV. Γ_T is shown for two choices of \mathcal{J} for the residual states. For the compound states, $\mathcal{J} = \mathcal{J}_r$. For both compound and residual states, $a = A/8 \text{ MeV}^{-1}$ and $\delta = 1.8 \text{ MeV}$.

TABLE III. Comparison of statistical-model calculations with experimental results. The same level-density parameter a was used for both compound and residual nuclei. The rigid-body value for the compound-nuclear moment of inertia was used throughout. The residual moment was varied as indicated below.

	Calculation		Experiment
	$a = A/7$	$a = A/8$	
I. Level density (MeV^{-1}) ($E^* = 34.2, J = 12$)	4.0×10^8	1.4×10^8	2.0×10^8
	$\mathcal{J} = \mathcal{J}_r$		
II. Compound-nuclear level width Γ (keV) (calculated values are for $J = 12$)	105	155	76 ± 17
	$\mathcal{J} = 0.75\mathcal{J}_r$		
III. Differential cross section at $\theta_{c.m.} = 90^\circ$ $d\sigma/d\Omega$ ($\mu\text{b}/\text{sr}$)	48	73	76 ± 17
	$\mathcal{J} = \mathcal{J}_r$		
$E = 36 \text{ MeV}$ $^{28}\text{Si}^+$	11.7	26.3	13.8 ± 1.4
2^+	20.2	45.5	18.7 ± 1.9
$E = 38 \text{ MeV}$ $^{28}\text{Si}^+$	14.5	30.9	12.0 ± 1.3
2^+	26.8	56.5	44.0 ± 4.0

describing the competing channels). The level density of the compound nucleus is not involved in this calculation.

The results of a statistical-model calculation are given by the solid curves in Fig. 7. For the reaction with 36.0-MeV incident ^{16}O ions leading to the ground state of the ^{28}Si residual nucleus, the shape of the calculated curve agrees roughly with the experimental data but is slightly out of phase in the region 10° – 40° ; and at intermediate angles (30° – 50°) the amplitude of the calculated cross-section oscillations is too small by almost a factor of 2. These observations indicate that the calculation includes the contribution from the proper compound-nuclear angular momentum states (predominantly $J_c = 12$ and 14), but that the relative contribution of these states is not entirely correct. Small adjustments of the optical-model parameters used (in particular the nuclear radii) may improve the fit. The calculated relative contributions of the different compound spin states as a function of compound-nuclear spin are illustrated for the ground state and first excited state of ^{28}Si in Fig. 8.

There are an infinite number of pairs of values of the level-density parameter a and moment of inertia \mathcal{J} which will reproduce the absolute magnitude of the cross sections. For example, in Fig. 7, a satisfactory fit to the data is obtained with $a = A/8$ and $\mathcal{J} = \mathcal{J}_r$. The region of a and \mathcal{J} space consistent with the experimental thick-target absolute cross sections at 90° c.m. for 36- and 38-MeV laboratory bombarding energies has been determined (Table III). For $\mathcal{J} = \mathcal{J}_r$, the a values are between $a = A/7$ and $a = A/9$. The fact that the differential cross sections cannot all be fit by the same parameters may be attributed partly to the experi-

mental error in the cross sections (which contributes an uncertainty in the fitted a value of approximately 10%) and the fact that the excitation energy region sampled (0.65 MeV c.m.) is insufficient to average out all of the cross-section fluctuations (see Fig. 1).

F. Results and Discussion of Statistical Calculations

The success of the statistical calculations is indicated by the agreement between the experimental and calculated quantities in Table III. The calculation of the compound-nuclear level density depends only on the level-density model and the parameters g , a , and δ . At the high excitation energies of this experiment a rigid-body moment of inertia is expected to best describe the compound nucleus. From Table III and Fig. 4, we find that $a=A/8$ and $g=g_r$ reproduce the experimental level density.

The calculations for the differential cross section depend on the residual level densities. Those for Γ depend on the residual and compound level densities. Because the compound decay populates residual states over a wide range of excitation energy, a rigid-body moment of inertia for the residual level density may not be appropriate. Calculations of Γ_α as a function of excitation in the residual state indicate that the peak of the residual population distribution (50% of the α decay) from compound states of $J=12$ is between 11–15 MeV of residual excitation energy. States reached by proton decay peak between 17–20 MeV. From Table III, values of $a=A/8$, $g=0.75g_r$ for the residual states and $g=g_r$ for the compound states reproduce the experimental Γ . The J dependence of Γ for α and proton decay using a representative set of level-density parameters is shown in Fig. 9.

As shown in Fig. 9, Γ is fairly independent of J if the residual state $g=g_r$. For $g=0.75g_r$, Γ drops sharply with J . A decrease in Γ with increasing J has been observed for the same compound system at lower energies.⁸ Calculations for Γ over a broad range of compound-nuclear excitation energies agree with experimental results from both light and heavy ion reactions (Fig. 6) if the residual $g=0.75g_r$. For residual $g=g_r$, the heavy ion results cannot be reproduced.

It is not expected that the experimental differential cross sections will be closely reproduced by the calculations. Several competing effects make the calculation of the differential cross sections quite sensitive to the transmission coefficients. As energy increases new, competing states become accessible to the decay process and tend to decrease the cross section to a given state. If the decay energy to a given state is below the combined Coulomb and centrifugal barriers, the transmission coefficients and hence the cross section to that state will tend to increase with energy. If the compound states of higher spin are reached as energy increases, the cross section to a given final state will tend to in-

crease, the amount of increase depending on the appropriate transmission coefficients. An investigation of the transmission coefficients used in this work indicates that these competing effects are indeed operative in the energy region investigated.

The experimental determinations of the differential cross sections may also be affected by Ericson fluctuations (the thick-target energy resolution being insufficient to completely damp the fluctuations) and the possible presence of nonstatistical reaction processes indicated by the fluctuation analyses.

From Table III, the calculated differential cross sections at 90° c.m. for $g=g_r$ and $a=A/8$ are roughly twice the experimental values. A change in the level-density parameter $a=A/7$ reduces the calculated results by a factor of 2. Using $g=0.75g_r$ increases the magnitude of the cross sections by a factor of 2 but does not alter the shape of the angular distribution. Because of the sensitivity of the cross sections to individual transmission coefficients as discussed above we consider the experimental values to be reproduced using parameters $a=A/7$ to $A/8$ and $g=0.75g_r-g_r$.

VII. SUMMARY

The angular distribution at 36 MeV laboratory bombarding energy shows that the $^{16}\text{O}(^{16}\text{O}, \alpha)^{28}\text{Si}$ ground-state reaction proceeds primarily through compound states having $J=12$. The predominant contribution from a single angular momentum state of the compound nucleus is supported by the angular cross-correlation fluctuation analysis. These observations are well accounted for by statistical-model calculations which exhibit the predominant contribution of high-spin states to this exit channel due to the difficulty in carrying away sufficient angular momentum when lighter particles are emitted. The density of $J=12$ levels in ^{32}S at 34.2 MeV of excitation energy has been found to be 2.0×10^8 levels/MeV. This value, as well as the absolute cross sections, are consistent with a level-density parameter $a=A/8$ to $A/7$.

In the fluctuation analysis of the thin-target excitation functions, there was some indication of cross correlation between α -particle emissions to the ground and first excited states of ^{28}Si . However, no correlation was found between the elastic scattering channel and the two α -emission channels in the fluctuation analysis. There is, however, an indication in Fig. 1 that at the highest energy both the elastic channel and all exit channels are in phase. Further work will be required to determine if a correlation will appear at higher energies than investigated in this study. The apparent absence in the energy region investigated of a correlation with the gross structure in elastic scattering is of interest, and indicates that the mechanism responsible for the gross structure in $^{16}\text{O}+^{16}\text{O}$ elastic scattering is different from that responsible for the structure previously observed

in $^{12}\text{C}+^{12}\text{C}$ elastic and reaction cross section at energies near the Coulomb barrier.³² The structure in the $^{12}\text{C}+^{12}\text{C}$ system at low energies has been interpreted in terms of "quasimolecular" states, and appeared in the elastic, α , proton, neutron, and γ exit channels.

Angular momentum effects may be playing a crucial role in determining the gross structure in the elastic scattering. It has been pointed out²⁸ that the peaks at 21, 25, and 29 MeV energy in the center of mass occur at the energies, where $l=14, 16,$ and 18 partial waves are expected to start contributing. It is also interesting to note that the structure observed by Siemssen *et al.* disappears at about the point ($E_{\text{c.m.}} \sim 32$) where the rotational energy associated with the maximum angular momentum expected ($J=20$) exceeds the available excitation energy of ^{32}S . It is not, however, possible to attribute the elastic scattering to a compound elastic process. The fluctuation analysis of the $^{16}\text{O}+^{16}\text{O}$ elastic scattering excitation function shows that compound elastic contributes less than 10% of the observed elastic cross section at 90° c.m. This is consistent with statistical-model calculations.

The fluctuation width deduced from the elastic and α -particle emission excitation functions is 76 ± 17 keV between 34.0 and 36.0 MeV of excitation energy in the ^{32}S compound nucleus. This width determination and those at lower energies are reproduced by statistical-model calculations using a level-density parameter of $A/8$ and a residual nuclear moment of inertia that is 0.75 of the rigid-body value. These calculations show a strong decrease in level width with increasing compound nuclear spin.

Note added in proof. Further thick target measurements have been made of the differential cross section in the elastic- and alpha-exit channels over the ^{16}O laboratory energy range 35–50 MeV in steps of 1 MeV. The elastic cross section was measured at 90° c.m. simultaneously with the alpha-emission cross sections to

³² E. Almqvist, D. A. Bromley, and K. A. Kuehner, *Phys. Rev. Letters* **4**, 515 (1960); D. A. Bromley, in *Enrico Fermi Summer School on Nuclear Structure and Nuclear Reactions*, Varenna, Italy, 1967 (unpublished).

the 0^+ ground and $2+$ first excited states in ^{28}Si at $70^\circ, 90^\circ, 110^\circ,$ and 120° c.m. There is no evidence for cross correlation between the alpha- and elastic-excitation functions at 90° c.m. The alpha-excitation functions exhibit a strong angular correlation indicative of contribution primarily from compound states of one or a few values of angular momentum.

At all angles there appears to be a significant cross-correlation between the 0^+ and $2+$ alpha-excitation functions as also was indicated in the thin target measurements over a narrower energy range reported above. These correlations clearly are not explained by the statistical fluctuation model; however, they do not necessarily fall outside the framework of the compound-nucleus-model assumptions as the following discussion will show.

As discussed by Ericson, the compound-nuclear-cross-section fluctuations are the result of (practically) random interference between many overlapping resonances in the compound system. Now, if two final states in the residual system are dynamically similar, it may be expected that the transition matrix elements between the coherent sums of amplitudes in the compound system and the final states will also be similar. The final states observed here are the 0^+ ground state and the $2+$ first excited state whose nature as a collective excitation built on the ground state has been well established. The difference in angular momentum between these states is not expected to be significantly restrictive in view of the fact that most of the alpha decay occurs from states of high angular momentum states in the compound nucleus. This example indicates the importance of distinguishing between the requirements of the compound-nucleus model and the more restrictive statistical fluctuation model.

ACKNOWLEDGMENTS

We thank Joanne Sauer for preparation of the targets used in this work. We also thank Dr. J. P. Bondorf, Dr. P. von Brentano, and Professor D. Bodansky for helpful discussions.